JOURNAL OF AIRCRAFT
Vol. 43, No. 5, September–October 2006

Engineering Notes

ENGINEERING NOTES are short manuscripts describing new developments or important results of a preliminary nature. These Notes should not exceed 2500 words (where a figure or table counts as 200 words). Following informal review by the Editors, they may be published within a few months of the date of receipt. Style requirements are the same as for regular contributions (see inside back cover).

Separation Control on a Trailing-Edge Flap Using Air Jet Vortex Generators

W. J. Crowther*
University of Manchester,
Manchester, M60 1QD, United Kingdom

Nomenclature

A	=	area
C_D	=	drag coefficient
C_L	=	lift coefficient
C_p	=	pressure coefficient
C_V	=	jet velocity ratio
C_μ	=	blowing coefficient (jet momentum ratio)
c	=	chord
DLG	=	flap deflection, lap and gap
f	=	jet orifice diameter
L	=	lift
M	=	Mach number
n	=	number of jets
p	=	static pressure
p_0	=	total pressure
q	=	freestream dynamic pressure
S	=	wing reference area
V	=	speed
x/c	=	nondimensional distance measured in a chordwise sense
α	=	angle of attack, or jet skew angle
β	=	jet pitch angle
γ	=	ratio of specific heats
Δ	=	flap deflection
λ	=	jet orifice spacing
ρ	=	density

Subscripts

j	=	jet
L	=	local
∞	=	freestream

I. Introduction

CIVIL-TRANSPORT aircraft are typically optimized for high-speed cruise and as a result require a high-lift system to obtain satisfactory performance at low speed.[1–4] High-lift-system design probably reached its peak of complexity at the end of the 1960s in the 747, which needed a three-element (triple-slotted) trailing-edge flap to get the required high-lift performance. Since then, civil-transport high-lift systems have tended to become simpler, with many current generation high-lift systems employing only a single-element flap.[5,6] The motivation for this is the pursuit of increased value through reduced manufacturing and maintenance costs rather than increased high-lift performance. However, in order to achieve acceptable performance with a single-element design, it is necessary to highly optimize the geometric location of the flap with respect to the main element trailing edge. This comes at the price of increased structural weight caused by increased structural stiffness of the flap tracks and actuation system. Within the present work, it proposed that by inclusion of flap flow control as part of the optimization process then equivalent performance can be achieved with relaxed geometric tolerances and therefore reduced weight and cost.

Traditional aerodynamic design is concerned with the arrangement of solid boundary conditions to optimize aerodynamic forces arising caused by fluid flow. With the availability of flow control technologies,[7] the designer also has the freedom to modify aerodynamic as well as geometric boundary conditions. Aerodynamic boundary conditions are modified by injection of momentum tangential to the flow direction, for example, circulation control via tangential blowing, or by providing means of redistributing the existing fluid momentum via the use of boundary-layer mixing devices, for example, vortex generators. Flow control devices such as vane vortex generators are routinely applied to production aircraft as flow fixes, and historically, circulation control has been applied to military high-lift systems. However, as yet, integrated flow control technologies have not seen wide application on civil high-lift systems, most probably because of the lack of suitable low-order models that can be used at the initial design stage.

II. Flow Control Strategy and Implementation

The flow control philosophy adopted in the present work is based on the enhancement of flap effectiveness through control of flap separation using air jet vortex generators (AJVGs). These devices enhance the mixing between the boundary-layer flow and freestream through production of streamwise helical structures and hence increase the momentum in the boundary layer close to the surface. In contrast to conventional vane vortex generators (VVGs), AJVGs enable improved penetration of the vortices through severe adverse pressure gradients by pumping excess momentum along the core of the vortices.[8] AJVGs also have the advantage that they impose minimal drag penalty when not in operation.

A major issue concerning the application of VGs of either type is in choosing appropriate location, spacing, and orientation.[9–14] There is general consensus amongs researchers that to be effective the AJVGs array must be located upstream of the region of flow to be controlled and that the most effective orientation is a pitch angle of 45 deg and skew angle of 90 deg. In terms of the pros and cons of co- or counter-rotating arrays, the effect of hole size with respect to the boundary-layer height, the spacing ratio of the holes with respect to the hole diameters, the picture is a little more mixed. For the present work, the AJVG implementation parameters are shown in Table 1. The orifice diameter was chosen on the basis that it was the smallest hole that could be drilled without specialist equipment and was reasonably close to the minimum hole size proposed from a fluidic efficiency point of view[15] (0.3 mm). The orifice spacing of 5 mm was chosen on the basis of previous (unpublished) experimental on the model using VVGs that had shown a spacing of 10 mm was effective.

Received 25 January 2005; revision received 11 April 2005; accepted for publication 12 April 2005.

*Senior Lecturer, School of Mechanical, Aerospace & Civil Engineering.

Table 1 AJVG implementation parameters

Fluid reference parameters		Geometric design parameters		Derived parameters	
Typical local flow speed	60 m/s	Orifice diameter ϕ	0.5 mm	Nondimensional orifice size ϕ/δ	0.5
Typical local boundary thickness d	1 mm	Orifice spacing λ	5 mm	Orifice spacing ratio λ/ϕ	10, 20, 40
Max jet speed	180 m/s	Pitch angle β	45 deg	Max jet velocity ratio	3
——	——	Skew angle α	90 deg	——	——
——	——	Rotation pairing and direction	Corotating, inboard	——	——

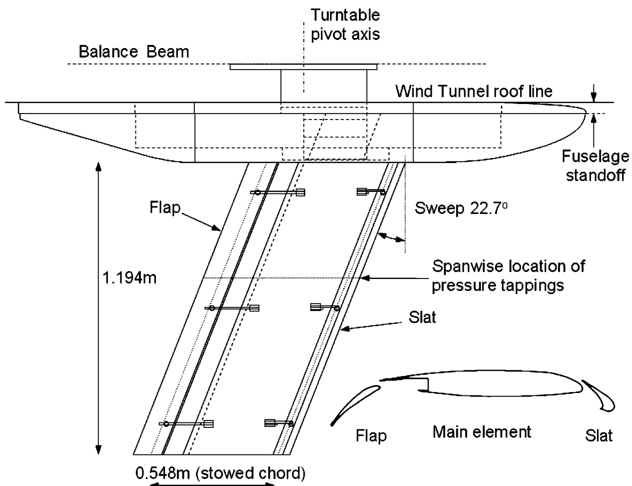

Fig. 1 Geometric details of the N56 swept panel high-lift model.

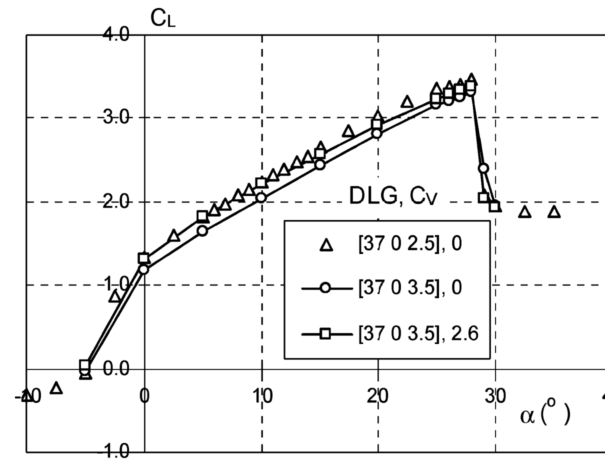

Fig. 2 Demonstration of the effectiveness of AJVGs in recovery of flap performance lost as a result of gap relaxation.

Five-mm spacing allows testing at 10- and 20-mm spacing through selective blocking of orifices. The VVG work had also shown that at a spacing of 10 mm a corotating array was more effective than a counter-rotating array.

III. Apparatus and Experimental Methods

A. Wind-Tunnel Model

The model consists of a single wing and half a fuselage and was mounted to the roof of the wind tunnel with the wing orientated vertically downwards (Fig. 1). The wing has a semispan of 1.194 m, a constant flap stowed chord of 0.548 m, and a sweep angle of 22.7 deg. The wing reference area is 0.654 m^2 based on the product of semispan and flap stowed chord. The fuselage is 2.5 m long and designed to provide representative flow around the root of the wing. Unless stated otherwise, all testing was carried out at a velocity of 30 m/s, giving a Reynolds number based on flaps stowed chord of around 1.1×10^6. The model has a three-element high-lift system consisting of main element, flap, and slat. The flap is of the single slotted Fowler type. When retracted, 66% of its 142-mm chord lies within the flap cove. The flap is mounted on three brackets and can be set at a number of discrete deflection settings. For the present work settings of 33, 37.5, 39.3, 42.7, 45.6, 47.6, and 50.6 deg were used. The brackets allow continuously variable positioning in terms of lap and gap. The design "optimal" settings for the flap are 33.1-deg deflection 0% lap and 2.5% gap. The slat, main element, and flap of the baseline model are pressure tapped at a spanwise station approximately 40% outboard of the fuselage. For ease of reference in the present experiments, the geometric setting of the flap is denoted by the three component vector $DLG = [\Delta \;\; lap \;\; gap]$, where $\Delta \in \{33, 37.5\}$, $lap = 0$, and $gap \in \{2.5, 3.5\}$. The wind tunnel is a closed-return facility with a maximum speed of 70 m/s and a working section freestream turbulence level of less than 0.1% at speeds up to 60 m/s. The balance y-axis limit load (lift) is 2 kN, and channel accuracy is of the order of 0.1% of full-scale deflection. The lift load on the model at $C_{L\max}$ and 30 m/s is approximately 50% of the balance full-scale deflection. Lift curves to $C_{L\max}$ at 30 m/s are repeatable to within plotting accuracy. The model spans 55% of the tunnel section. Wind-tunnel corrections were not applied to the data presented in this paper.

B. Data Reduction

Two different independent parameters are used to characterize the actuation effort. The first is the jet velocity ratio C_V, defined as the ratio of the jet velocity to the local freestream velocity in the region of the jet exit. The second is the blowing momentum coefficient C_μ, defined as the ratio of the jet momentum to freestream reference momentum. These parameters are defined as follows:

$$C_V = \frac{V_j}{V_L} = \frac{M_j}{M_L} = \left\{ \frac{p_{0,j}[(\gamma-1)/\gamma] - p_L}{p_{0,\infty}[(\gamma-1)/\gamma] - p_L} \right\}^{\frac{1}{2}} \tag{1}$$

and

$$C_\mu = \frac{\rho_j n A_j V_j^2}{\frac{1}{2}\rho_\infty A_{\text{ref}} V_\infty^2} \tag{2}$$

If the flow is assumed to be incompressible, then the two flow parameters are related as follows:

$$C_\mu = \frac{\rho_j n A_j (1 - C_p)}{\frac{1}{2}\rho_\infty A_{\text{ref}}} C_V^2 \tag{3}$$

The dependent parameters of lift, drag, and pressure were nondimensionalized in the normal manner.

IV. Results

A. Force Data

As a demonstration of the basic effectiveness of AJVGs in recovering the flap performance lost caused by gap relaxation, Fig. 2 shows the lift curves for three separate cases: first, the baseline design optimum case of [37.5 0 2.5] with no blowing; second, the relaxed gap case [37.5 0 3.5] with no blowing, and third, the same relaxed gap case with blowing at a C_V of 2.6. Overall, these results clearly show that the flap performance of the relaxed gap case has been substantially recovered by the application of blowing. Note that a previous (unpublished) study using the same model has shown that results of similar form can be obtained using VVGs; however, the (unoptimized) performance was around 70% down on the AJVG performance.

To establish a more detailed picture of the effectiveness of the AJVGs, tests were performed for range of flap deflections up to 51 deg and for C_V values up to 2.8 at 0-, 5-, and 10-deg angle of

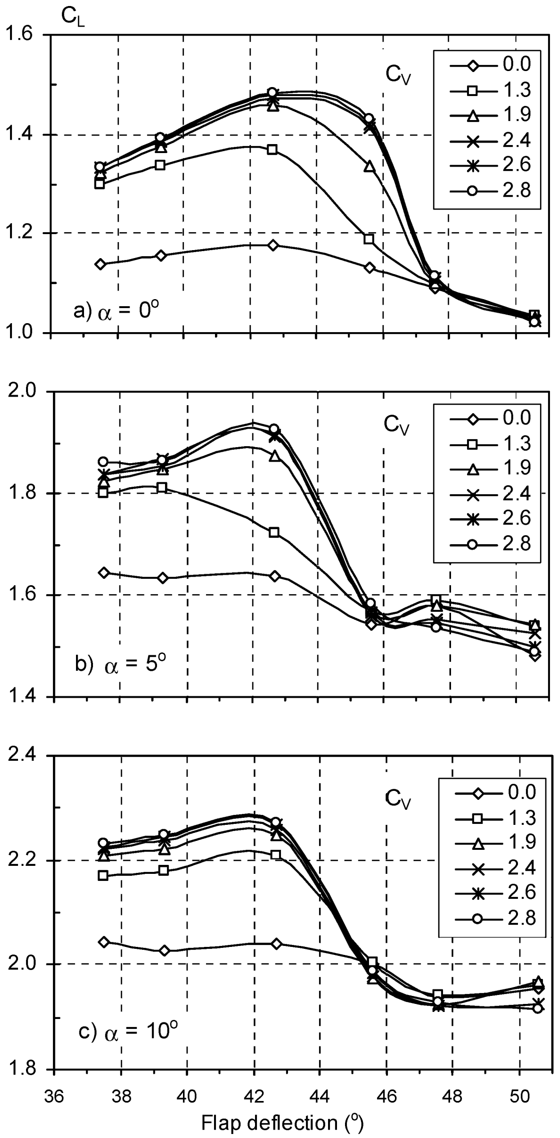

Fig. 3 Flap performance recovery due to blowing for increasing flap deflection at 0-, 5-, and 10-deg angle of attack.

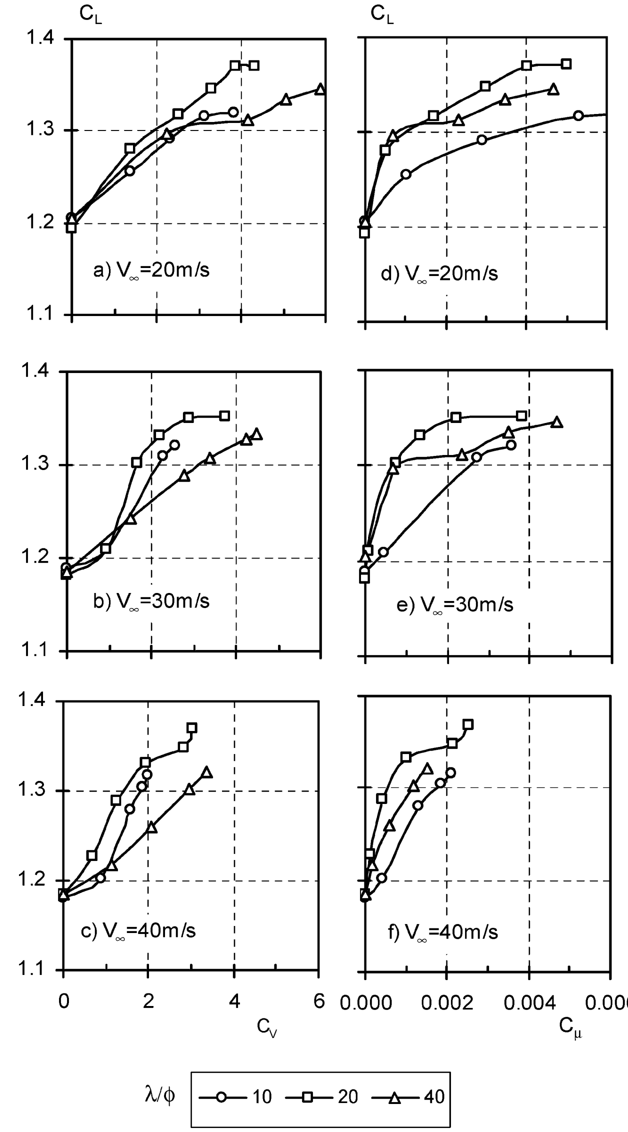

Fig. 4 Effect of orifice spacing on lift recovery: left-hand column, C_L plotted against jet velocity ratio; right-hand column, C_L plotted against jet momentum coefficient. DLG = [37 0 3.5], and α = 0 deg. Orifice diameter is 0.5 mm.

attack (Fig. 3). The results for each of the angles of attack are all similar in form. For lower flap deflections, increasing C_V increases the overall lift of the configuration; however, above a certain flap deflection, increasing C_V has zero effect, indicating that the flap separation has moved ahead of the actuator array.

The effect of freestream speed and jet orifice spacing on the blown performance of the model is shown in Fig. 4. The left-hand column shows C_L plotted against C_V and the right-hand column shows C_L plotted against C_μ. Considering the C_V results first, it can be seen that the overall form of the results is similar for different speeds. This confirms that it is reasonable to use C_V as a similarity parameter for the present work. Looking now at the effect of orifice spacing, it is clear that a spacing ratio of 20 produces results with the highest gain, that is, the largest change in C_L for a given C_V, with the spacing ratio of 10 in second place. The maximum effectiveness of flap separation control is effectively limited by complete reattachment of flow on the flap and thus should be independent of orifice spacing. The results presented here tentatively support this; however, further data at high C_V and high freestream speed are needed to reach a definite conclusion.

The results plotted against C_μ are a little harder to interpret because changing the spacing changes the overall orifice area and therefore changes C_μ for a given velocity ratio; however, they give an indication of comparative gain of the various spacings based on the amount of momentum required. Once again it appears that the spacing ratio of 20 gives the best gain; however, interestingly the spacing ratio of 40 comes in second place. From a momentum perspective, it is clearly more efficient to use fewer orifices running at high C_V than it is to use more orifices running at low C_V.

B. Flow Visualization

Surface oil-flow-visualization results comparing the flap upper-surface flow pattern for blowing on and blowing off for the [37 0 3.5] test case are shown in Fig. 5. Considering the unblown case first (Fig. 5a) it can be deduced that the flow separates approximately 5% x/c downstream from the jet orifice array. With blowing applied (Fig. 5b), the separation line has to move back to approximately 90% x/c from the leading edge. This figure also shows evidence of streakline downstream of the jet orifices, typical of the patterns that would be expected for a longitudinal vortex embedded in the boundary sublayer. These surface streaklines curve in a direction spanwise towards the wing tip eventually asymptoting to the separation line. This behavior is consistent with previous studies of vortex-generating devices ahead of a 3d separation line.

V. Scaling Considerations

The practicality of flow control schemes using blowing often hinges on the amount of engine bleed air required for their operation.

Table 2 Reference data for the Airbus A320

Parameter	Value
Gross weight	74,000 kg
Wing span	34 m
Wing reference area	122 m^2
%span of trailing-edge flap	80
Power plant	CFM56-5, 120 kN thrust
Number of engines	2
Mass flow per engine at takeoff	386 kg/s
Mass flow per engine, landing	38.6 kg/s
Approach speed	70 m/s
Local C_p on flap at around 30% x/c	−3

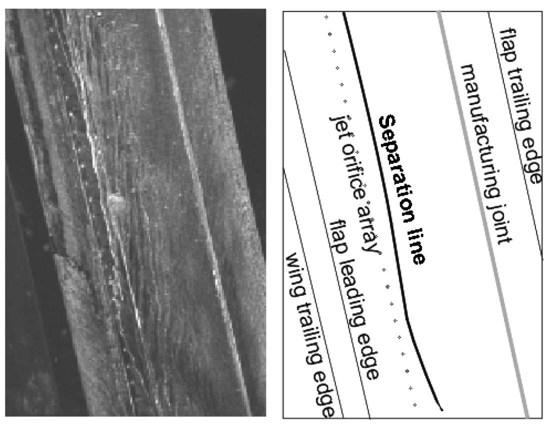

a) Baseline (no blowing)

b) Blowing on C_V = 2.6

Fig. 5 Surface oil-flow visualization of the flow over the upper surface of the flap comparing the separation location for blowing on and blowing off. DLG = [37.5 0 3.5], α = 0 deg, and V_∞ = 30 m/s. Flow from left to right.

To put experimental air requirements in to context, what follows is an approximate calculation of the engine bleed requirements if the present experimental rig were scaled up in size and speed to an Airbus A320 aircraft (Table 2). The bleed air requirements are calculated using two different methods. The first method is based simply on using the same hole diameter, spacing, and velocity ratio on the full-scale flap as on the model flap. The second method is based on the assumption that the momentum requirements can be scaled for a different wing area and freestream speed using the blowing coefficient. A maximum jet exit velocity of 280 m/s ($M = 0.82$) is imposed as a constraint in both cases. Values are calculated approximately using Eq. (3) under the assumption of incompressible flow.

The results for the velocity ratio scaling and for momentum ratio scaling are presented in Tables 3 and 4, respectively. The input values for the calculation are in italics, and the significant output values are in bold. A jet velocity ratio of 2 is chosen as a representative

Table 3 Blown air requirements based on jet velocity ratio scaling

Parameter	Value
Jet velocity ratio	*2*
Orifice diameter	*0.5 mm*
Hole spacing ratio	*20*
Orifice spacing	10 mm
Total number of jets on flap	2720
Total orifice area	5.34×10^{-4} m^2
Jet velocity	280 m/s
Jet mass flow	0.18 kg/s
Jet momentum	50.3 N
Jet mass flow as a % of engine mass flow, landing	**0.46%**
Jet momentum as a % of engine thrust, landing	**0.21%**

Table 4 Blown air requirements based on jet momentum coefficient scaling

Parameter	Value
Jet momentum coefficient	*0.00115*
Orifice diameter	*8.23 mm*
Hole spacing ratio	*20*
Orifice spacing	160 mm
Total number of jets on flap	661
Total orifice area	5.34×10^{-4} m^2
Jet velocity	280 m/s
Jet mass flow	2.95 kg/s
Jet momentum	827 N
Jet mass flow as a % of engine mass flow, landing	**7.65%**
Jet momentum as a % of engine thrust, landing	**3.45%**

value from the present experimental work. This corresponds with a blowing coefficient of 0.00115 at 30 m/s, model scale, and a hole spacing ratio of 20. If the results are scaled simply by velocity ratio, then an A320 scale application of the present flap flow control scheme would require a mass flow equal to 0.46% of the available engine mass flow and a momentum flow equal to 0.21% of the overall thrust during landing. Alternatively, if the results are scaled by momentum ratio, then the requirement would be a mass flow equal to 7.65% of the available engine mass flow and a momentum flow equal to 3.45% of the overall thrust for the same condition. Note that in order to keep the jet velocity below 280 m/s for the momentum scaling case, it has been necessary to greatly increase the hole size beyond what is likely to be practical.

VI. Conclusions

This paper has outlined the design requirements for civil-transport high-lift systems and made a case that value could be increased by the use of flow control to allow relaxation of the high-lift system positional tolerances without loss in overall performance. Experimental work using a swept panel high-lift model has identified that relaxation of the flap gap from 2.5 to 3.5%c at a flap deflection of 37.5 deg led to an approximately 0.2 drop in C_L over the useful angle range of the high-lift system. Surface flow-visualization studies have shown that this loss in performance caused by separation of the flap upper-surface boundary layer. The application of flow control in the form of AJVGs approximately 30% x/c from the leading edge of the flap running at a C_V of 2.6 enabled reattachment of the flap upper-surface boundary layer and hence recovery of the original flap performance. Experiments at increased flap deflection demonstrated that the performance boundaries defined by the proposed flow control model are valid. Investigation of the effect of actuator spacing showed that a hole spacing ratio of 20 gave the best system gain. At experimental scale, results collapse reasonably well with speed using C_V or C_μ as the similarity parameter. Provisional scaling of the experimental results to an A320 type aircraft indicate that approximately 0.5% of engine landing mass flow would be required based on a velocity ratio scaling and 8% based on momentum ratio scaling.

Acknowledgments

The research reported here was undertaken as part of the AEROMEMS II project (Advanced Aerodynamic Flow Control using MEMS, Contract G4RD-CT-2002-00748). Thanks are extended to Tim Harrison for providing the baseline wind-tunnel data and Steven Kendall for the blown data.

References

[1]Smith, A. M. O., “High-Lift Aerodynamics,” *Journal of Aircraft*, Vol. 12, No. 6, 1975, pp. 501–530.

[2]Nield, B. N., “An Overview of the Boeing 777 High Lift Aerodynamic Design,” *Aeronautical Journal*, Nov. 1995, pp. 361–371.

[3]Flaig, A., and Hilbig, R., “High-Lift Design for Large Civil Aircraft,” Advisory Group for Aerospace Research and Development (AGARD) CP-515, Paper 31, Neuilly Sur Seine, France, Sept. 1993, pp. 1–12.

[4]Rudolph, P. K. C., “High-Lift Systems on Commercial Subsonic Transport Aircraft,” NASA CR-4746, Sept. 1996.

[5]Wedderspoon, J. R., “The High Lift Development of the A320 Aircraft,” Proceedings of the 15th International Council of the Aeronautical Sciences (ICAS), London, 1986, pp. 343–351.

[6]Hansen, H., “Overview About the European High Lift Research Programme Eurolift,” AIAA Paper 2004-767, Jan. 2004.

[7]Gad-El-Hak, M., “Introduction to Flow Control,” *Flow Control-Fundamental an Practices*, edited by M. Gad-El-Hak, A. Poolard, and J. P. Bonnet, Springer-Verlag, Berlin, 1998, pp. 1–107.

[8]Lewington, N. P., Peake, D. J., Henry, F. S., and Singh, C., “Analogue/Digital Wind Tunnel Testing of Active Low Momentum Flow Control on Single and Multi-Component Airfoil Systems at High Lift,” AIAA Paper 2002-0303, Jan. 2002.

[9]Lin, J. C., “Review of Research on Low-Profile Vortex Generators to Control Boundary Layer Separation,” *Progress in Aerospace Science*, Vol. 38, No. 4–5, 2002, pp. 399–401.

[10]Suzuki, T., Nagata, M., Shizawa, T., and Honami, S., “Optimal Injection Conditions of a Single Pulsed Vortex Generator to Promote Cross-Stream Mixing,” *Experimental Thermal and Fluid Science*, Vol. 17, No. 1-2, 1998, pp. 139–146.

[11]Magill, J. C., and McManus, K. R., “Exploring the Feasibility of Pulsed Jet Separation Control for Aircraft Configurations,” *Journal of Aircraft*, Vol. 38, No. 1, 2001, pp. 48–56.

[12]Rae, A. J., Galrin, S. A., and Fulker, J., “Investigation into the Scale Effects on the Performance of Sub Boundary Layer Vortex Generators on Civil Aircraft High-Lift Devices,” AIAA Paper 2002-3274, June 2002.

[13]Lin, J. C., “Review of Research on Low-Profile Vortex Generators to Control Boundary Layer Separation,” *Progress in Aerospace Science*, Vol. 38, No. 4–5, 2002, pp. 399–401.

[14]Barberopoulos, A. A., and Garry, K. P., “The Effect of Skewing on the Vorticity Produced by an Airjet Vortex Generator,” *The Aeronautical Journal*, Vol. 102, No. 1009, March 1998, pp. 171–177.

[15]Ho, C. H., and Tai, Y. U., “Micro-Electro-Mechanical-Systems (MEMS) and Fluid Flow,” *Annual Review of Fluid Mechanics*, Vol. 30, 1998, pp. 579–612.